



**Fermi National Accelerator Laboratory**

**FERMILAB-Conf-98/023-E**

**CDF**

**R and D Results for the Proposed  
Intermediate Fiber Tracker of CDF**

Juan A. Valls

For the CDF Collaboration

*Rutgers, The State University of New Jersey  
Piscataway, New Jersey 08855-0849*

*Fermi National Accelerator Laboratory  
P.O. Box 500, Batavia, Illinois 60510*

January 1998

Published Proceedings of *SCIFI97, Conference on Scintillating and Fiber Detectors*,  
University of Notre Dame, November 3-7, 1997

## **Disclaimer**

*This report was prepared as an account of work sponsored by an agency of the United States Government. Neither the United States Government nor any agency thereof, nor any of their employees, makes any warranty, expressed or implied, or assumes any legal liability or responsibility for the accuracy, completeness, or usefulness of any information, apparatus, product, or process disclosed, or represents that its use would not infringe privately owned rights. Reference herein to any specific commercial product, process, or service by trade name, trademark, manufacturer, or otherwise, does not necessarily constitute or imply its endorsement, recommendation, or favoring by the United States Government or any agency thereof. The views and opinions of authors expressed herein do not necessarily state or reflect those of the United States Government or any agency thereof.*

## **Distribution**

*Approved for public release; further dissemination unlimited.*

## **Copyright Notification**

*This manuscript has been authored by Universities Research Association, Inc. under contract No. DE-AC02-76CHO3000 with the U.S. Department of Energy. The United States Government and the publisher, by accepting the article for publication, acknowledges that the United States Government retains a nonexclusive, paid-up, irrevocable, worldwide license to publish or reproduce the published form of this manuscript, or allow others to do so, for United States Government Purposes.*

# R&D Results for the Proposed Intermediate Fiber Tracker of CDF

Juan A. Valls

*Rutgers, The State University of New Jersey  
for the CDF collaboration*

**Abstract.** In this paper, R&D results for the proposed Intermediate Fiber Tracker detector for the CDF upgrade are presented. We show a detailed study of the performance of the tracker under the high radiation levels expected during the Tevatron Run II operation. The system is proved to be highly efficient even after the expected  $2 \text{ fb}^{-1}$  of delivered luminosity. A rate capability study has also been conducted on readout SSPM to address the issue of high rate operation. High efficiency is well maintained up to several MHz expected for Run II.

## INTRODUCTION

Fermilab is currently facing a major challenge with the operation of the Run II Tevatron collider. The accelerator structure will be enhanced by the fall of 1999 with the inclusion of the Main Injector. Anticipated instantaneous luminosities of up to  $2 \times 10^{32} \text{ cm}^{-2} \text{ s}^{-1}$  and bunch crossings of 132 ns will require a major upgrade for the CDF and D detectors. This represents a major change with respect to the past Tevatron operation where maximum instantaneous luminosities of  $1.7 \times 10^{31} \text{ cm}^{-2} \text{ s}^{-1}$  with 3.5  $\mu\text{s}$  bunch interval times were reached.

CDF is in the process of a tracking system upgrade to accommodate the higher luminosities and shorter bunch crossing times planned for Run II. The silicon vertex detector (SVX) will be replaced with a 5-layer, double-sided system (SVX II) much longer along the beam axis and with a pipeline readout. The original Central Tracking Chamber (CTC) will be replaced with a new Central Outer Tracker (COT) with a similar open cell structure but four times smaller drift distances. For the space between the SVX II and the COT (approximately between 19 and 40 cm) a fine granularity scintillating fiber detector was originally proposed, referred to as the Intermediate Fiber Tracker (IFT). The IFT detector consists of 12 doublet layers (6 axial and 6 stereo) of 800  $\mu\text{m}$  diameter scintillating fibers. The length of the fibers vary from 180 to 300 cm and cover the pseudorapidity range  $|\eta| < 2$ . Each of the fibers is connected to a 0.8 mm clear fiber which is routed through the gap between the central structure and the end-plug calorimeter to the outer

surface of the detector structures, where Visible Light Photon Counters (VLPC's) are housed in liquid helium cryostats.

## LIGHT YIELD

Several factors affect the light yield transmission of scintillating fibers. These are:

- the scintillating fiber length,  $L_{sc}$ , and its attenuation length,  $\lambda_{sc}$ ,
- the clear fiber length,  $L_{cl}$ , and its attenuation length,  $\lambda_{cl}$ ,
- the mirror reflectivity,  $R$ , if the far end of the fiber is mirrored,
- the connector efficiency,  $\epsilon_{conn}$ , between scintillating and clear fibers, if they are spliced together,
- the cassette transmission efficiency,  $\epsilon_{cass}$ , from the clear fibers to the readout VLPC (Visible Light Photon Counter), and
- the quantum efficiency of the VLPC,  $QE$ .

The light transmission may then be written as:

$$T = \left[ \exp\left(-\frac{z}{\lambda_{sc}}\right) + R \exp\left(-\frac{2L_{sc} - z}{\lambda_{sc}}\right) \right] \epsilon_{conn} \exp\left(-\frac{L_{cl}}{\lambda_{cl}}\right) \epsilon_{conn} \epsilon_{cass} QE \quad (1)$$

where  $z$  is the distance between the particle track and the connector to the clear fiber (near end).

## Attenuation Length

A systematic measurement of the attenuation length of both scintillating and clear fibers of various diameters and types has been performed at Fermilab within the CDF group [1]. The type of fibers included standard 3HF (1% PTP, 1500 ppm) and fibers with slightly different 3HF derivatives. Fibers from both Kuraray and Bicron were used. 3HF and clear fibers were spliced together and placed in a dark box. Scintillating fibers were then illuminated with a UV lamp and light yield was measured by a photodiode at the end of the clear fibers. The measured attenuation curves were well fitted by single exponentials for both 3HF type fibers and clear fibers. The results are shown in Fig. 1 and Fig. 2. In the case of 3HF fibers there is no diameter dependence among the fibers. The clear fibers showed a mild dependence on the diameter.

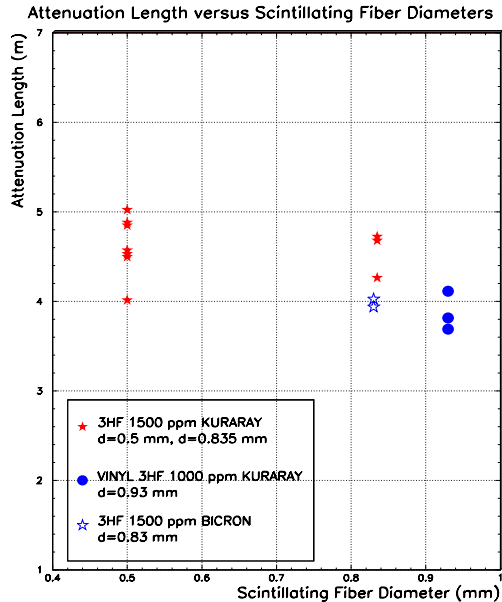


FIGURE 1. Attenuation length vs fiber diameter for scintillating fibers.

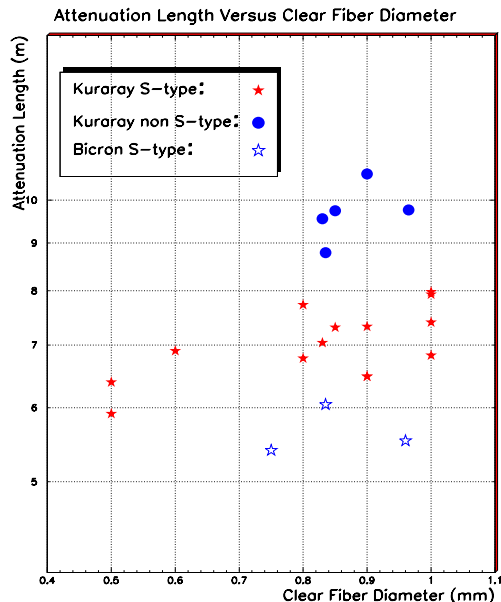


FIGURE 2. Attenuation length vs fiber diameter for clear fibers.

## RADIATION DAMAGE

Light transmission in plastic optical fibers is known to suffer from radiation exposure. The radiation hardness of plastic fibers has been reported by the the D group [2] in the range of 100 krad and above. More recently, the University of Tsukuba group at CDF extended these measurements to a lower range, from 700 krad to 0.4 krad for both 3HF (1% PTP, 1500 ppm) scintillating and clear fibers [3]. The fibers used in this study were Kuraray multicladd s-type fibers of 0.5-0.75 mm diameter for 3HF and 0.8 mm for clear fibers. A  $^{60}\text{Co}$   $\gamma$ -source was utilized to irradiate the fibers at different radius ( $R=12, 35$  and  $75$  cm). More irradiation results have also been obtained when using a  $^{137}\text{Cs}$   $\gamma$ -source and fast neutrons at the JINR pulsed reactor in Dubna [4].

The light output degradation of 3HF fibers can be attributed to the degradation of the attenuation length and not to the scintillating mechanism itself. The radiation hardness of both scintillating and clear fibers is identical if expressed in terms of the ratio of attenuation lengths before and after irradiation, and it is well described as a linear function of  $\log_{10}$  of dose. The results are shown in Fig. 3.

### Expected Degradation and Radiation Dose Profile

The radiation level in the IFT can be estimated using the radial dose profile measured with the CDF SVX' detector during the 1992-93 run [5]. The dose mea-

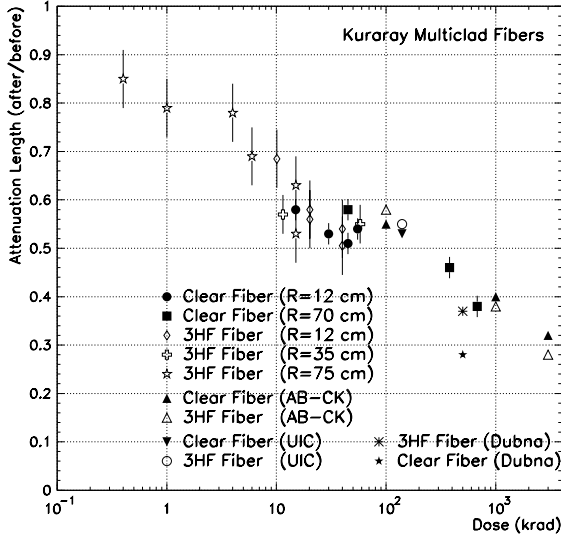


**FIGURE 3.** Ratio of attenuation lengths before and after irradiation. Measurements AB-CK (A. Bross, C. Kim) and UIC are taken from [1].

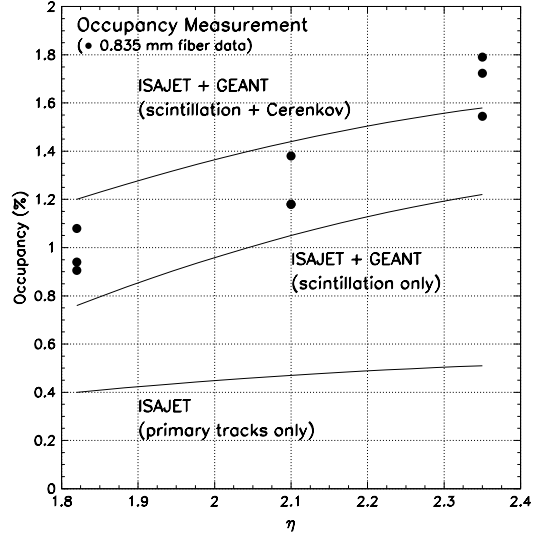


**FIGURE 4.** Comparison of the occupancy measured by 0.8 mm scintillating fibers and Monte Carlo simulation results.

sured with a dosimeter was  $300 \text{ rad/pb}^{-1}$  for the SVX layer 0 ( $r=3 \text{ cm}$ ). A radial dependence of  $r^{-1.7}$  was found from the increase in the leakage current measured for layers 0 to 3 ( $3 < r < 8 \text{ cm}$ ). Extrapolating the dose profile to the inner ( $r=19 \text{ cm}$ ) and outer ( $r=40 \text{ cm}$ ) layers of the proposed system, radiation doses of 24 and 7.3 krad are expected, respectively, for  $2 \text{ fb}^{-1}$  delivered luminosity during Run II.

Another way to evaluate the light yield drop due to radiation damage is to estimate the dose profile using Monte Carlo. The dose profile in the CDF Run II environment has been evaluated using a complete ISAJET + full GEANT simulation [6]. The energy deposition in the fibers was translated into dose using the measured inelastic  $p\bar{p}$  cross section and the charged multiplicity distribution ( $dN/d\eta = 4.5$ ). A realistic calibration of the simulation was provided by the measurement made with 3HF fibers inserted into the CDF detector in the last Run 1C in 1996 [7]. A bundle of 16 scintillating fibers of different lengths and diameter were placed at a radius of 27 cm and readout by 8 m long clear fibers with Solid State Photomultipliers (SSPM's). The measured occupancy is compared with the predictions of the simulation in Fig. 4. Considering the uncertainty in the Cerenkov contribution produced in the clear fibers strung through the  $10^\circ$  hole of the endplug calorimeter, there is good agreement between the data and the simulation results.

Fig. 5 shows the simulation results for the dose profiles along the fibers [6]. The distribution is essentially flat along the  $z$ -direction. The dose over the length of the cylindrical part of the innermost layer at  $r = 21 \text{ cm}$  is  $\sim 22 \text{ krad}$  for  $2.5 \text{ fb}^{-1}$

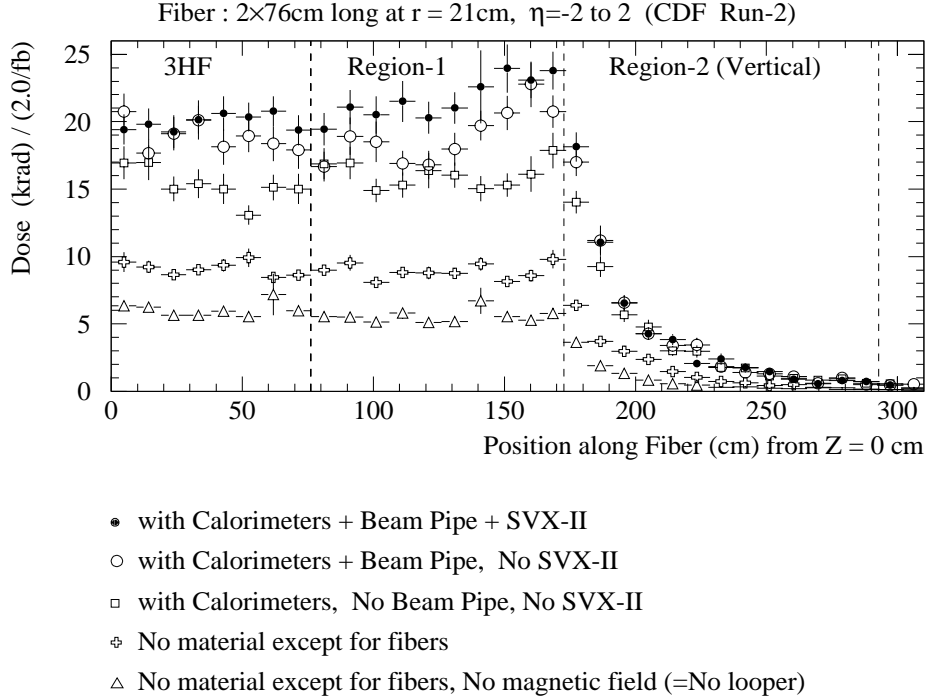


**FIGURE 5.** Dose profile evaluated for  $2 \text{ fb}^{-1}$ . The abscissa corresponds to the fiber length from  $z = 0$ . The fiber is parallel to the beam ( $L < 1.6 \text{ m}$ ), routed between the COT and the end-plug calorimeter ( $1.6 < L < 2.5 \text{ m}$ ).

reasonably consistent with the value extrapolated from the SVX measurement. A significant enhancement of the background due to low energy particles looping in the magnetic field, electron pairs converted from photons and back splash from the end-plug calorimeters is seen.

Taken this expected behavior to model the light yield transmission along the fibers, Fig. 6 shows the overall transmission of a signal generated at the middle of the tracker ( $\eta = 0$ ). Two curves ( $R=0.9$  and  $R=0.8$ ) are shown for the two conditions considered before and after  $2.5 \text{ fb}^{-1}$  of integrated luminosity. The right-handed side scale indicates the expected number of photoelectrons. This number has been estimated from several measurements done within the CDF group [8] and found in agreement, within uncertainties, with the observed number by the D group with their cosmic ray test stand [9] as the realistic basis.

Fig. 7 shows the efficiency of each doublet layer as a function of the average number of photoelectrons per single fiber. Doublet layer efficiencies above 99.5% for  $\geq 6 \text{ PE}$  indicate that the proposed IFT has an operational margin greater than 50% even at the weakest point at  $\eta = 0$ .

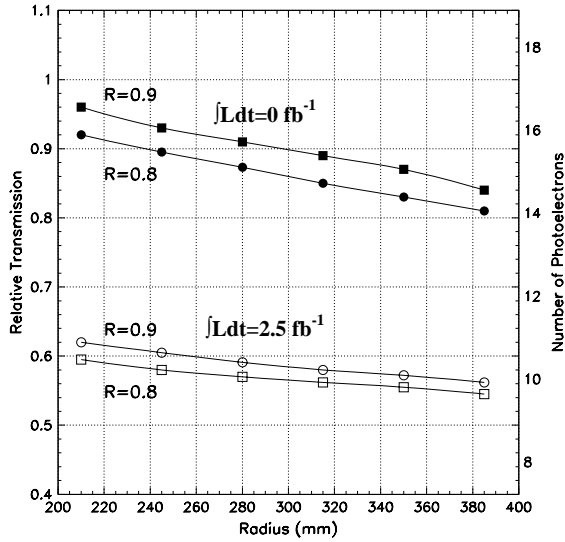


**FIGURE 6.** Relative transmission and expected number of photoelectrons for signals generated at the middle point of the tracker before and after integrating  $2.5 \text{ fb}^{-1}$  of delivered luminosity.

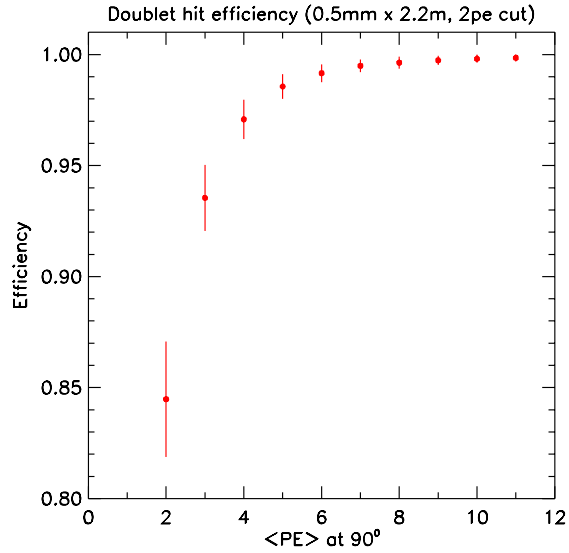


**FIGURE 7.** Doublet layer hit efficiency as a function of the average number of photoelectrons per single fiber.

## OCCUPANCY AND PHOTOELECTRON RATE

A study of the rate capability of SSPM [10] and VLPC [11] has been performed within the CDF collaboration to address the issue of the performance of these read-out devices under high rate operation. The setup used is similar to the originally developed by D [12]. For the case of the SSPM measurement, light from two laser diodes<sup>1</sup> illuminated the input connector of a cassette holding four 8-channel SSPM cells. The 32-channel cassette was suspended in a liquid helium cryostat. The light emission spectrum from the diodes peaks at 635 nm, well within the broad peak of the SSPM's. One of the diodes, referred to as “background”, was excited by a pulse train with frequencies between 100 kHz and 6 MHz. This pulse height generated about 2 photoelectrons and was intermittent with a frequency of 100 Hz, as shown in Fig. 8. A 2 ms pause was imposed after every 8 ms. During this pause, the second diode, referred as “signal” was fired with a variable “quiet time” after the last pulse of the background pulse train.

Data was taken for the set of parameters shown in Table 1. For each set of parameters the pulse height spectra of the SSPM output was fit with the following formula:

<sup>1)</sup> Hitachi HL6314MG.

**TABLE 1.** Parameter sets for the rate capability measurement.

Temperature	Bias voltage, $V_{bias}$
7.5 K (72 k $\Omega$ )	-6.0 V
6.9 K (86 k $\Omega$ )	-6.5 V
6.5 K (96 k $\Omega$ )	-6.5 V, -7.0 V
6.0 K (112 k $\Omega$ )	-7.0 V, -7.5 V

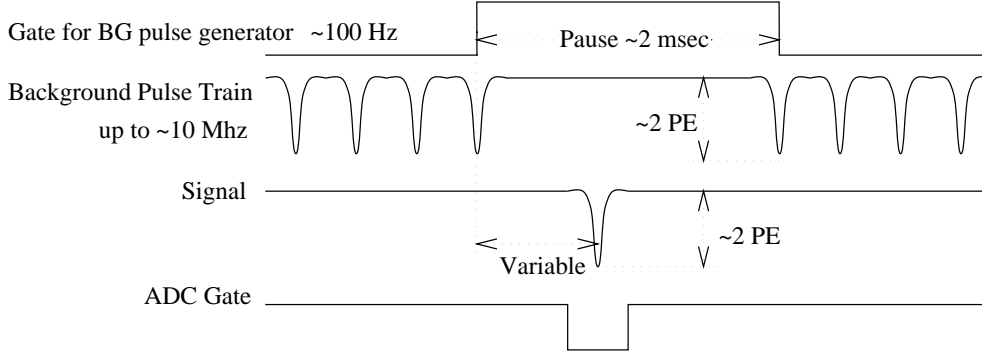


**FIGURE 8.** Timing diagram for the rate capability test.

$$S(q) = \sum_{n=0}^{\infty} S_n(q) = N \sum_{n=0}^{\infty} G_n(q) \frac{(\overline{N_{pe}})^n}{n!} e^{-\overline{N_{pe}}}$$

$$G_n(q) = \frac{1}{\sqrt{2\pi}\sigma_n} \exp \left[ -\frac{1}{2} \left( \frac{q - p - n \cdot g}{\sigma_n} \right)^2 \right] ; \quad \sigma_n = \sqrt{\sigma_p^2 + n \cdot \sigma_{gain}^2}$$

where  $p$  is the pedestal,  $\sigma_p$  its Gaussian spread,  $g$  the average gain of avalanches,  $\sigma_{gain}$  its spread, and  $\overline{N_{pe}}$  the average number of PE's. The Gaussian spread of the peaks and the gain, which is the incremental distance between the peaks, are assumed to be the same among all peaks. The gain is linear and the fit is excellent within the measured pulse height range, as shown in Fig. 9 and Fig. 10 for single PE rates of 220 kHz and 11 MHz, respectively.

The number of photoelectrons, which is interpreted as a quantum efficiency in relative scale, increases with both the temperature and the bias voltage and, in both cases, this behavior is more significant at high rates. No sizable dependence of the pedestal position is observed on the temperature and bias voltage at low rates. However, at higher frequencies there is a striking decrease of the pedestal position towards higher values of the temperature and bias voltage.

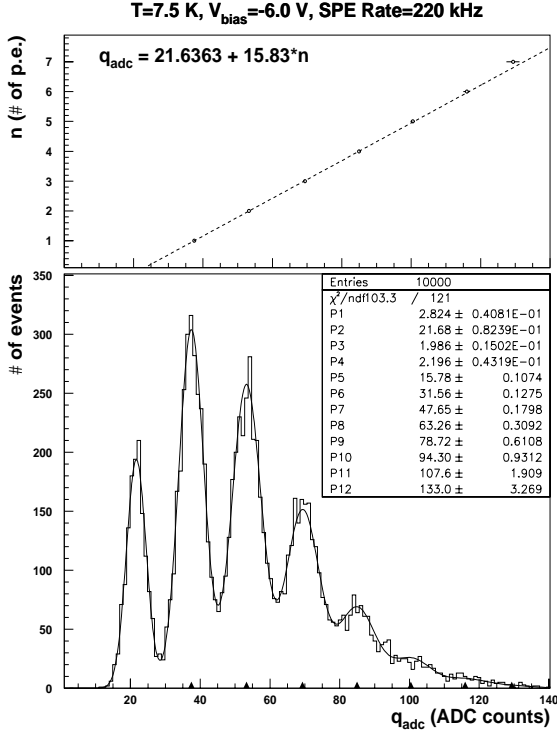


**FIGURE 9.** Number of photoelectrons (top) and pulse height distribution (bottom) for a single PE rate of 220 kHz.

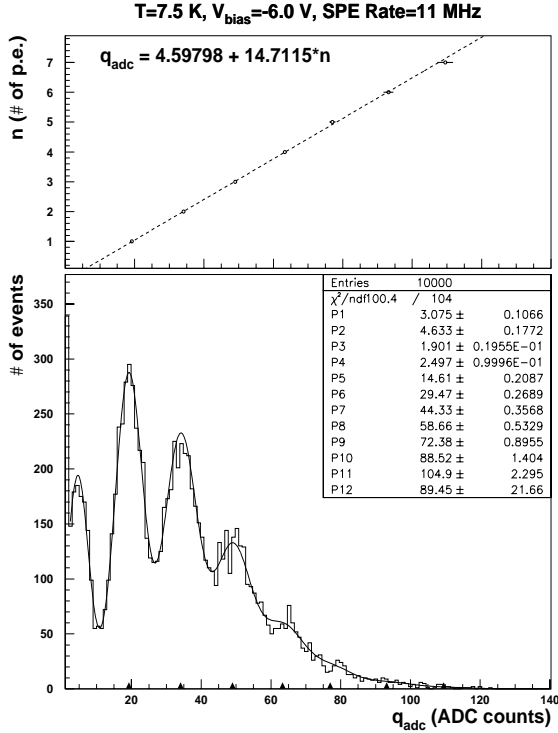


**FIGURE 10.** Number of photoelectrons (top) and pulse height distribution (bottom) for a single PE rate of 11 MHz.

Within the tested range of the operating conditions, Figure 11 shows a gradual decrease of the gain with the single PE rate above 1 MHz. This decrease in gain at high frequencies is slightly improved by increasing the temperature. In these ideal conditions the gain reduction is only a few percent. The quantum efficiency seems to be even less affected by the increase of rate and no visible effect can be noticed up to 4 MHz SPE rate, as shown in Figure 11. Above this rate, an overall trend of decrease is observed below several percent level up to 12 MHz.

## CONCLUSIONS

A fine granularity scintillating fiber tracking system was proposed for the intermediate radial range of the CDF detector. A detailed study of its performance, specially under the high rate conditions of Run II, has proved the detector to be highly efficient for integrated luminosities of up to  $2 \text{ fb}^{-1}$ . The rate capability of SSPM has also been studied for various combinations of temperature and bias voltage. Using a laser diode flasher, measurements were made up to a single photoelectron rate of 12 MHz. Only a slight decrease, less than several per cent, of the

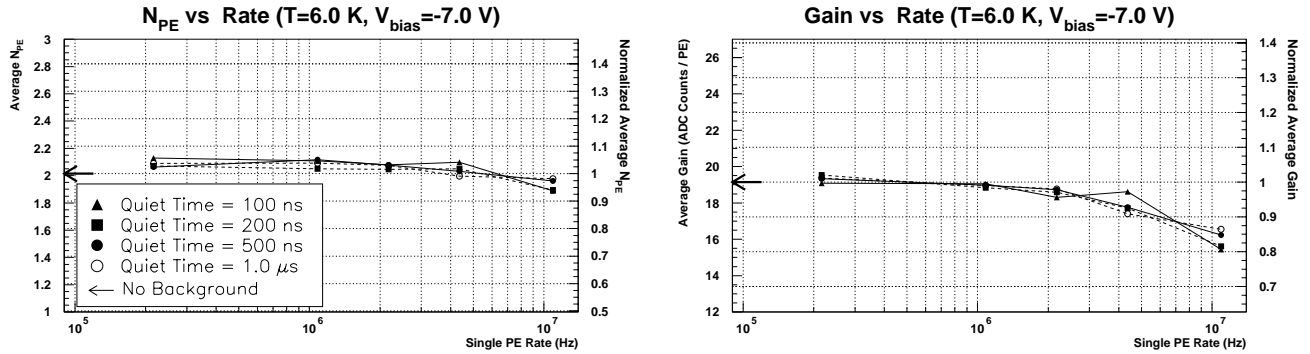


FIGURE 11.  $\overline{N_{pe}}$  and gain vs single PE rate for T=6.0 K and  $V_{bias}=-7.0$  V.

quantum efficiency was observed at this rate whereas a 10% drop of the gain was observed.

## ACKNOWLEDGEMENTS

I would like to thank the organizers of the conference for the excellent work. My sincere thanks also for prof. M. Atac, M. Mishina and F. Bedeschi for let me participate in this project and the large experience gained by working with them.

## REFERENCES

1. D. Cassettari *et al*, Measurement of Attenuation Length of Scintillating and Clear Fibers, CDFnote 3560, February, 1996.
2. S. Margulies *et al*, Proceedings of SCIFI 93 Workshop on Scintillating Fiber Detectors, World Scientific, pp. 421-430, October 1993.
3. K. Hara *et al*, Radiation Hardness of Kuraray Optical Fibers, CDFnote 3727, June 25, 1996.
4. F. Bedeschi *et al*, Radiation Hardness of New Kuraray Double Cladded Optical Fibers, CDFnote 3583, March, 1996.
5. P. Azzi *et al*, Noise and Radiation Effects on SVX' and Other Silicon Sensors, CDFnote 3278, August 1995.  
M. A. Frautschi, Radiation Damaga Issues for the SVXII Detector, CDFnote 2368, January, 1994.
6. T. Yoshida, private communication.
7. G. Bolla, R. Demina, Measurement of the Intermediate Fiber Tracker Occupancy, CDFnote 3623, June 1996.
8. M. Atac *et al*, Measurement of the Light Yield from 0.5 mm Scintillating Fibers with the IFT prototype, CDFnote 3569, April 1996.

- R. Demina *et al.*, Measurement of the Relative Photoelectron Yield of 0.5 mm and 0.835 mm Scintillating Fibers, CDFnote 3559, February, 1996.
9. D. Adams *et al.*, Cosmic Ray Test Results of the D Prototype Scintillating Fiber Tracker, Fermilab-Conf-95/012-E, January, 1995.
10. J. A. Valls *et al.*, Study of the Performance of SSPM's at High Rate, CDFnote 3790, July, 1996.
- M. Gubinelli *et al.*, Measurement of the Rate Capability of Solid State Photomultipliers Using Visible Light, Fermilab-PUB-97-104, April, 1997, submitted to Nucl. Instr. and Meth.
11. F. Bedeschi *et al.*, Measurement of VLPC Gain and Q.E. as a Function of Pulsing Rate, CDFnote 3752, January, 1997.
12. J. Warchol, *these proceedings*.